

# Initial conditions of urban permeable surfaces in rainfall-runoff models using Horton's infiltration

Steffen Davidsen, Roland Löwe, Nanna H. Ravn, Lina N. Jensen and Karsten Arnbjerg-Nielsen

## ABSTRACT

Infiltration is a key process controlling runoff, but varies depending on antecedent conditions. This study provides estimates on initial conditions for urban permeable surfaces via continuous simulation of the infiltration capacity using historical rain data. An analysis of historical rainfall records show that accumulated rainfall prior to large rain events does not depend on the return period of the event. Using an infiltration-runoff model we found that for a typical large rain storm, antecedent conditions in general lead to reduced infiltration capacity both for sandy and clayey soils and that there is substantial runoff for return periods above 1–10 years.

**Key words** | Horton, infiltration, initial conditions, runoff, urban

**Steffen Davidsen** (corresponding author)  
**Roland Löwe**  
**Karsten Arnbjerg-Nielsen**  
Department of Environmental Engineering,  
Technical University of Denmark,  
Bygningstorvet, Bygning 115, 2800 Kgs. Lyngby,  
Denmark  
E-mail: [stda@env.dtu.dk](mailto:stda@env.dtu.dk); [stda@ramboll.dk](mailto:stda@ramboll.dk)

**Nanna H. Ravn**  
**Lina N. Jensen**  
LNH-Water,  
Kathøjvej 3, 3080 Tikøb,  
Denmark

## INTRODUCTION

In an urban context, impermeable surfaces are the primary contributors to runoff (Fletcher *et al.* 2013; Redfern *et al.* 2016) but permeable surfaces are increasingly used in urban areas as an adaption strategy to changing precipitation patterns. Runoff from permeable areas is therefore becoming more important to consider, especially during rain events with high intensity. However, runoff from permeable surfaces depends on several physical processes that are difficult to describe (Chahinian *et al.* 2005; Ogden *et al.* 2011). Urban hydrologists therefore often describe runoff from permeable surfaces with substantially simplified models or completely neglect it (e.g., Chahinian *et al.* 2005; Leandro *et al.* 2016).

According to Gregory *et al.* (2006) and Pitt *et al.* (2008), compaction is common for urban soils and significantly decreases the infiltration capacity. The reduction in infiltration capacity causes an increase in frequency, volume and peak flow of runoff from permeable surfaces (Pitt *et al.* 1999; Gregory *et al.* 2006), highlighting the necessity of including runoff from permeable surfaces in urban runoff models. The additional runoff from permeable surfaces may influence extent and frequency of surcharges, overflows and flooding in the catchment, both for short rainstorms with high intensity and for longer rains with large volume.

Infiltration is an important process in the assessment of runoff from permeable surfaces. Along with the physical soil properties, the water content strongly affects infiltration rates. The water content in the beginning of a rain event depends on the antecedent conditions and varies from event to event, unlike the physical properties. This leads to uncertainty on the amount of runoff that should be expected from permeable areas, for example, when applying design storms for hydraulic simulations of the urban water system. The purpose of this study is therefore to assess the degree to which infiltration rates in the beginning of major rain events vary in time and for different soil types, leading to improved accuracy of urban runoff modelling.

## METHODS AND DATA

To study the dynamics of the infiltration process, we considered historical rainfall records and analysed

- (i) the accumulated precipitation prior to a large number of major rain events and
- (ii) the infiltration conditions in the beginning of the events, based on continuous simulations of the rainfall-infiltration-runoff process using a Horton approach.

## Rainfall records

We have considered continuous rainfall records from SVK station 5740 (Kløvermarksvej) in Copenhagen, Denmark. Data were available for the period from 1979 to 2012 in 1-minute resolution. For our analysis, we identified 71 rain events with return periods greater than 0.5 years based on the one-hour maximum intensity (Madsen et al. 2017). The 10 largest rain events are summarized in Table 1 and describe the characteristics of large rain events in this region. For the remainder of this paper, we base the return period on the 1-hour maximum intensity, since the analysis in this paper is particularly important for simulations with design storms, which are typically used for hydraulic dimensioning with heavy rainfall.

## Modelling infiltration and runoff

An infiltration-runoff model similar to those applied in commercial models, such as MOUSE (DHI 2014) and KOSIM (ITWH 2009), is set up in order to simulate the infiltration process. The model for describing infiltration capacity and runoff is based on Horton's and modified Horton's equations (Horton 1941; Verma 1982).

$$f_p = f_c + (f_0 - f_c) \cdot e^{-k \cdot t} \quad (1)$$

$$f_p = f_0 - (f_0 - f_c) \cdot e^{-k_i \cdot (t - t_w)} \quad (2)$$

Horton's equation (Equation (1)) describes the decline in infiltration capacity  $f_p$  from the maximum capacity  $f_0$  to the minimum capacity  $f_c$ , with the decrease parameter  $k$

and is applicable when rain intensity exceeds the infiltration capacity. The Modified Horton's equation (Equation (2)) describes the increase in infiltration capacity using the increase parameter  $k_i$  during dry periods and  $t_w$  the time where  $f_p = f_c$ . Neither of these equations is valid when the precipitation rate is below infiltration capacity. Thus, like KOSIM, the model setup is based on a mass balance for the water depth  $y$  on the surface which is replenished by the precipitation depth  $p$  and depleted by the infiltration depth  $f$ .

Excess water on the surface leads to the formation of runoff. The model equations are summarized in Table 2 and variables are explained in Table 3. Four cases are considered, corresponding to dry and wet conditions (Case I and IV), as well as transition periods where either the initial losses are filled or depleted (Case II), or where infiltration occurs and the precipitation rate is smaller than the infiltration capacity (Case III). We consider infiltration as continuous; i.e., the total infiltration volume is not limited.

## Evaluation of infiltration conditions in the start of major rain events

Using the model described in the previous section, we perform a simulation of the infiltration process with a warm-up period of 14 days. As infiltration rates strongly depend on the characteristics of the soil, we carry out multiple simulations using the different soil types shown in Table 4. In particular, we perform simulations for both compacted and non-compacted soils, as many permeable areas in cities are frequently used for recreational purposes and thus must be assumed to be compacted.

**Table 1** | Data on rain events used in simulations

Return period (1 hr-based)	>1,000	51.8	34.5	26.4	15.3	11.3	10.1	7.9	7.5	6.4
Return period (24 hr-based)	1,000	13.1	1.47	42.0	1.24	4.51	2.30	0.53	10.4	0.61
Event start	2011 2 Jul. 16:54	2001 6 Aug. 19:18	2008 11 Jul. 03:51	1986 24 Jul. 09:45	1997 30 Jun. 16:28	1998 3 May 18:07	2008 8 Aug. 12:04	2004 24 Aug. 21:21	2008 4 Aug. 00:04	2003 24 May 20:06
Duration [min]	170	492	63	426	128	204	130	155	461	82
Rain in event [mm]	118.8	53.20	31.40	68.80	29.00	42.00	25.60	24.00	43.80	22.60
Max 1 min precipitation [mm]	3.00	1.40	3.40	1.20	2.40	1.00	1.60	1.80	1.00	1.20
Max 30 min precipitation [mm]	54.00	25.20	30.00	17.80	16.21	14.60	15.00	14.80	15.80	13.44
Max 1 hour precipitation [mm]	94.20	35.00	31.37	29.20	25.20	23.20	22.53	21.10	20.80	19.90
Max 24 hour precipitation [mm]	138.40	53.20	32.80	68.80	31.60	42.00	36.20	26.20	50.56	27.00

Return periods are specified based on both maximum 1-hour intensity and maximum 24-hour intensity (Madsen et al. 2017).

**Table 2** | Processes and governing equations within each case

Case number Case description	I Dry condition	II Wetting/Drying	III Transition period	IV Wet condition
Case identifier(s)	$p(t) = 0 \ \& \ y(t) = 0$	$0 < (y_{(t-1)} + p(t)) < y_{ws}$	$y_{(t-1)} \geq y_{ws} \ \& \ p(t) \leq f(t)$	$(y_{rs,(t-1)} + p(t)) > f(t)$
Initial water depth (at beginning of time step)	0	$y(t) = y_{(t-1)} + p(t)$	$y(t) = y_{ws} + p(t) + y_{rs,(t-1)}$	$y(t) = y_{ws} + p(t) + y_{rs,(t-1)}$
Infiltration capacity, $f_p$	$f_{p(t)} = f_0 - (f_0 - f_{p(t-1)}) \cdot e^{-k_i \cdot \Delta t}$	$f_{p(t)} = f_0 - (f_0 - f_{p(t-1)}) \cdot e^{-k_i \cdot \Delta t}$	$f_{p,i} = f_c + (f_{p(t-1)} - f_c) \cdot e^{-k \cdot t_i}$ $f_{p(t)} = f_0 - (f_0 - f_{p,i}) \cdot e^{-k_i \cdot t_r}$	$f_{p(t)} = f_c + (f_{p(t-1)} - f_c) \cdot e^{-k \cdot \Delta t}$
Infiltration depth, $f$	-	-	If $p(t) > \int_0^{t_i} f_p(t) dt$ : $f(t) = \int_0^{t_i} f_p(t) dt$ for $f_p \in [f_c, f_0]$ If $p(t) \leq \int_0^{t_i} f_p(t) dt$ : $f(t) = p(t)$	$f(t) = \int_0^{\Delta t} f_p(t) dt$ for $f_p \in [f_c, f_0]$
Surface water depth, $y_s$ (water depth available for runoff)	-	-	$y_{s(t)} = y(t) - y_{ws} - f(t)$	$y_{s(t)} = y(t) - y_{ws} - f(t)$
Runoff, $Q$	-	-	$Q(t) = M \cdot B \cdot I^{1/2} \cdot y_s^{5/3}(t)$	$Q(t) = M \cdot B \cdot I^{1/2} \cdot y_s^{5/3}(t)$
Water depth (surface), $y_{rs}$ (water remaining on surface after runoff and infiltration)	-	-	$y_{rs(t)} = y_{s(t)} - \frac{Q(t) \cdot \Delta t}{A}$	$y_{rs(t)} = y_{s(t)} - \frac{Q(t) \cdot \Delta t}{A}$
Final water depth, $y$ (at end of time step)	0	If $p > 0$ (wetting): $y(t) = y_{(t-1)} + p(t)$ If $p = 0$ (drying): $y(t) = y_{(t-1)} - 0.0005 \frac{m}{hr} \cdot \Delta t$	$y(t) = y_{ws} + y_{rs(t)}$	$y(t) = y_{ws} + y_{rs(t)}$
Additional functions	-	-	$t_i = \frac{p(t)}{f(t)} \cdot \Delta t, \ t_r = \Delta t - t_i$	-

Description of variables can be found in Table 3.

**Table 3** | Descriptions of parameters in the infiltration-runoff model

Variable	Description	Unit	Variable	Description	Unit
$p$	Precipitation depth	$L$	$F$	Accumulated infiltration depth	$L$
$y$	Water depth	$L$	$t$	Time step (current)	–
$y_{ws}$	Water depth of initial losses	$L$	$t - 1$	Previous time step	–
$y_s$	Water depth available for runoff (potential runoff depth)	$L$	$\Delta t$	Length of time step	$T$
$y_r$	Actual runoff depth	$L$	$t_i$	Duration with infiltration	$T$
$y_{rs}$	Surface water depth	$L$	$t_r$	Duration without infiltration (recovery)	$T$
$f$	Infiltration depth	$L$	$Q$	Runoff flow	$L^3/T$
$f_p$	Infiltration capacity (infiltration velocity)	$L/T$	$M$	Manning number	$L^{1/3}/T$
$f_0$	Maximum infiltration capacity	$L/T$	$B$	Width of channel	$L$
$f_c$	Minimum infiltration capacity	$L/T$	$I$	Slope	–
$k$	Capacity decrease exponent	$T^{-1}$	$A$	Area	$L^2$
$k_i$	Capacity increase exponent	$T^{-1}$			

Infiltration parameters for the different soil types are obtained from the literature, and include both measured values and values from modelling studies. For the parameter sets where no initial losses are specified, we assume a wetting depth of  $5 \cdot 10^{-5}$  metres and a storage depth of  $1 \cdot 10^{-3}$  metres (DHI 2014). Drying times of 2–3 and 10 days were considered for sandy and clayey soils, respectively (Rossman & Huber 2016).

To compare infiltration conditions for the different soil types, we consider the relative infiltration capacity  $f_{p,rel}$  as a measure of the currently available infiltration capacity:

$$f_{p,rel} = \frac{(f_p - f_c)}{(f_0 - f_c)} \cdot 100\% \quad (3)$$

The sensitivity of runoff to the initial conditions is investigated by additional runoff simulations. In these simulations, the infiltration capacity at the beginning of the rain event is specified as either the maximum or minimum infiltration capacity of the corresponding soil type.

To compute the maximum potential runoff  $Q_{tot,max}$  from an event, we consider:

$$f_{p(0)} = f_c \quad (4)$$

To compute the minimum potential runoff  $Q_{tot,min}$  from an event, we consider:

$$f_{p(0)} = f_0 \quad (5)$$

**Table 4** | Collection of Horton infiltration parameters from literature

	Initial (maximum) infiltration capacity, $f_0$ [m/s]	Final (minimum) infiltration capacity, $f_c$ [m/s]	Capacity decrease exponent, $k$ [ $s^{-1}$ ]	Capacity increase exponent (recovery), $k_i$ [ $s^{-1}$ ]	Reference
Clayey soils					
Clayey top soil (Charlottenlund Fort, Copenhagen)	$2.57 \times 10^{-5}$	$4.17 \times 10^{-6}$	$9.72 \times 10^{-3}$	–	Dybkjær et al. (2016)
Compacted clayey soil	$2.40 \times 10^{-5}$	$2.82 \times 10^{-6}$	$3.7 \times 10^{-3}$	$3.23 \times 10^{-6}$ to $6.47 \times 10^{-6}$	Pitt et al. (1999)
Sandy soils					
Compacted sandy soil	$1.06 \times 10^{-4}$	$1.27 \times 10^{-5}$	$7.02 \times 10^{-3}$	$1.51 \times 10^{-5}$	Pitt et al. (1999)
Non-compacted sandy soil	$2.75 \times 10^{-4}$	$1.06 \times 10^{-4}$	$6.7 \times 10^{-3}$	$2.26 \times 10^{-5}$	Pitt et al. (1999)
Mean					

All models use a drying rate of  $1.39e-7$  m/s for recovery of initial losses from DHI (2014).

## RESULTS AND DISCUSSION

### Accumulated rain depth prior to major rain events

Figure 1 shows the percentage of rain events where accumulated precipitation prior to the event is lower than a given threshold for four different durations before the events and for three different classes of return periods. While precipitation prior to an event is subject to random variability, the figure suggests that prior rainfall does not depend on the return period of the considered rain event. To support this conclusion, we applied the two-sided Wilcoxon rank sum tests (Hollander & Wolfe 1973). In total, 12 tests were performed using the function 'wilcox.test' in R (R Core Team 2015), performing pairwise comparisons for the three potential combinations of data sets for different return periods that were repeated for each of the four considered durations before the rain events. The p-values of the 12 tests range from 0.16 to 0.95 and are thus clearly bigger than the commonly applied significance level of 0.05. The tests can thus not identify any significant differences in the distributions of pre-event rainfall for the different return periods.

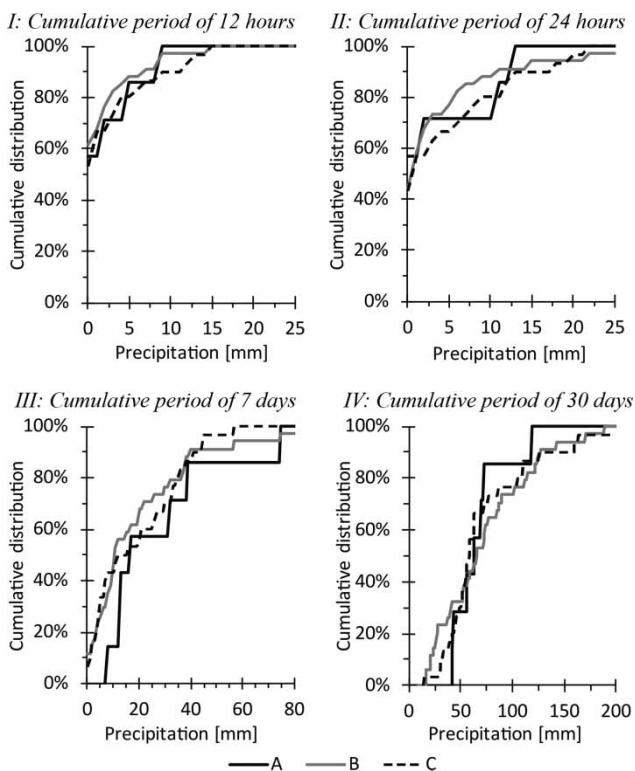


**Figure 1** | Percentage of rain events where accumulated precipitation prior to the event is less than a given threshold. Shown for different durations before the event (subfigures I–IV) and for events with different return periods T (A (black): T > 10 years, B (grey): T = 1–10 years, C (black, dashed): T = 0.5–1 years).

### Infiltration capacity for historical rain events

Figure 2 illustrates the relative infiltration capacity in the start of rain events as a function of return period, as well as the percentage of rain events where the relative infiltration capacity is below a certain threshold. There is a significant variation of relative infiltration capacities for both types of sandy and clayey soil. Considering clayey soils, the relative infiltration capacity in the start of an event is lower than 50% for approximately half of the events. Even for sandy soils, 25% of the events start with significantly reduced relative infiltration capacities of 70% or less. This implies that assuming infiltration capacity to be fully available in the start of a simulated design storm leads to overly optimistic results in many cases. The results shown in Figure 2 can be used to define realistic initial conditions reflecting the required level of safety, e.g., covering at least 90% of the events.

### Impact of initial conditions in surface runoff

Figure 3(a) shows the total runoff depth for the considered events, comparing runoff for 100% impermeable areas and permeable areas with compacted clayey and sandy soils. Total runoff from the permeable areas seems to vary mostly as a function of the return period, independent of the total rainfall depth of an event. There is no runoff from sandy soils at return periods below 10 years. Runoff from clayey soils begins for return periods of less than 1 year, but at very low rates.

Figure 3(b) shows the maximal hourly runoff rate simulated during the different events as a function of the return period of the events. As the return period of the events was determined based on hourly rainfall intensities, the dependency would be expected to be smooth. This is also apparent from the runoff rates shown for impervious areas in Figure 3(b). For permeable areas, we observe significant variations in the maximal hourly runoff rate for events with similar return periods. For clayey soils, these variations are in the order of 3–6 mm for return periods less than 10 years, corresponding to 15–20% of the maximal hourly rainfall depth or 30–50% of the maximal runoff depth from the permeable areas. Even for compacted sandy soils, variations of the maximal runoff rate in the order of 7 mm are observed for stronger rain events, highlighting the importance of initial infiltration conditions for the simulated runoff.

Figure 4 illustrates the sensitivity of the simulated runoff to the assumed infiltration capacity in the beginning of an event, by comparing how simulated runoff would differ

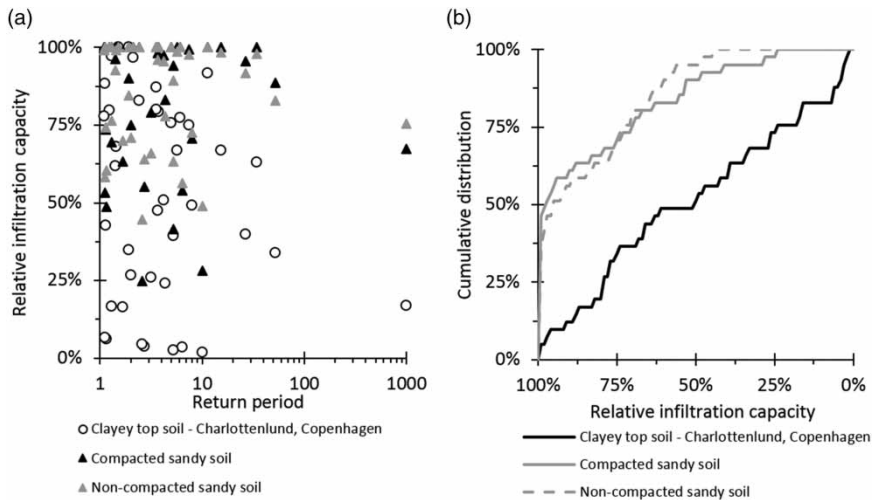


**Figure 2** | (a) Relative infiltration capacity at start of large rain events for sandy and clayey soils for events with different return periods. (b) Cumulative distribution of the relative infiltration capacity in (a).

from the value obtained from continuous simulations ( $Q_{tot,acc}$ ), when assuming either minimal ( $Q_{tot,max}$ ) or maximal ( $Q_{tot,min}$ ) infiltration capacity in the start of an event. For clayey soils, we observe the largest variations at low return periods (Figure 4(a) and 4(b)) due to the generally small infiltration capacities of these soils. The differences between  $Q_{tot,acc}$  and  $Q_{tot,min}$  as well as  $Q_{tot,max}$  are of similar magnitude and in the order of few millimetres. This suggests that for these soil types an appropriate representation of initial infiltration conditions is important for events below or within the design range of the urban water system. For larger events the variation in runoff resulting from the initial infiltration conditions is less relevant, as the variation is small compared to the total runoff. Interestingly, the sensitivity of simulated runoff from clayey soils to the initial

infiltration conditions is of similar magnitude as the uncertainty of observed runoff from impervious surfaces, which was estimated to have a standard deviation of 2 mm (Arnbjerg-Nielsen & Harremoës 1996).

For compacted sandy soils we observe that the runoff obtained from the continuous simulation largely corresponds to  $Q_{tot,max}$  and that the sensitivity of simulated runoff to initial conditions seems less dependent on return period (Figure 4(c)). The largest difference between  $Q_{tot,max}$  and  $Q_{tot,acc}$  occurs for the event registered on 11 July 2008 and is due to a very high rainfall intensity at the very beginning of the event. In a practical sense, our results suggest that it is safe to assume that compacted sands can allow water to infiltrate at their maximum capacity in the beginning of an event.

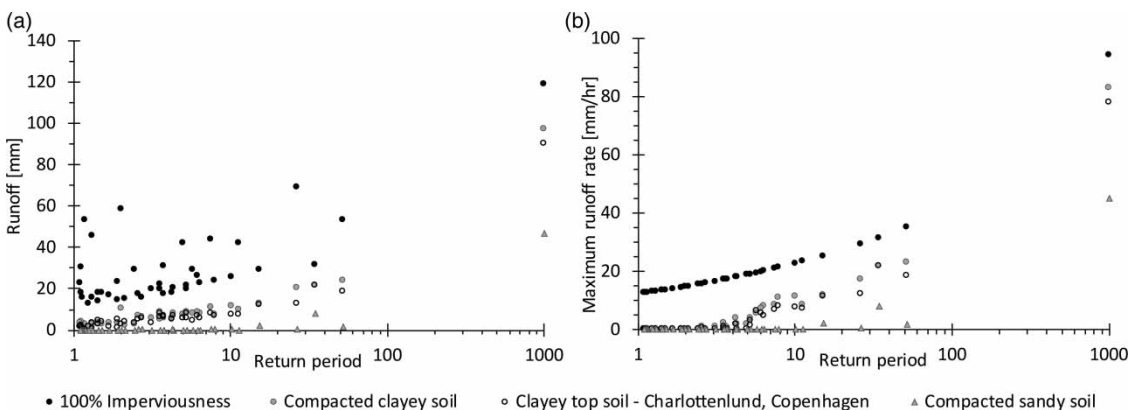


**Figure 3** | (a) Simulated total runoff depth for historical rain events with return periods based on the maximum hourly rain intensity. There is no simulated runoff from non-compacted sandy soils. (b) Simulated maximum hourly runoff rate for the same historical rain events.

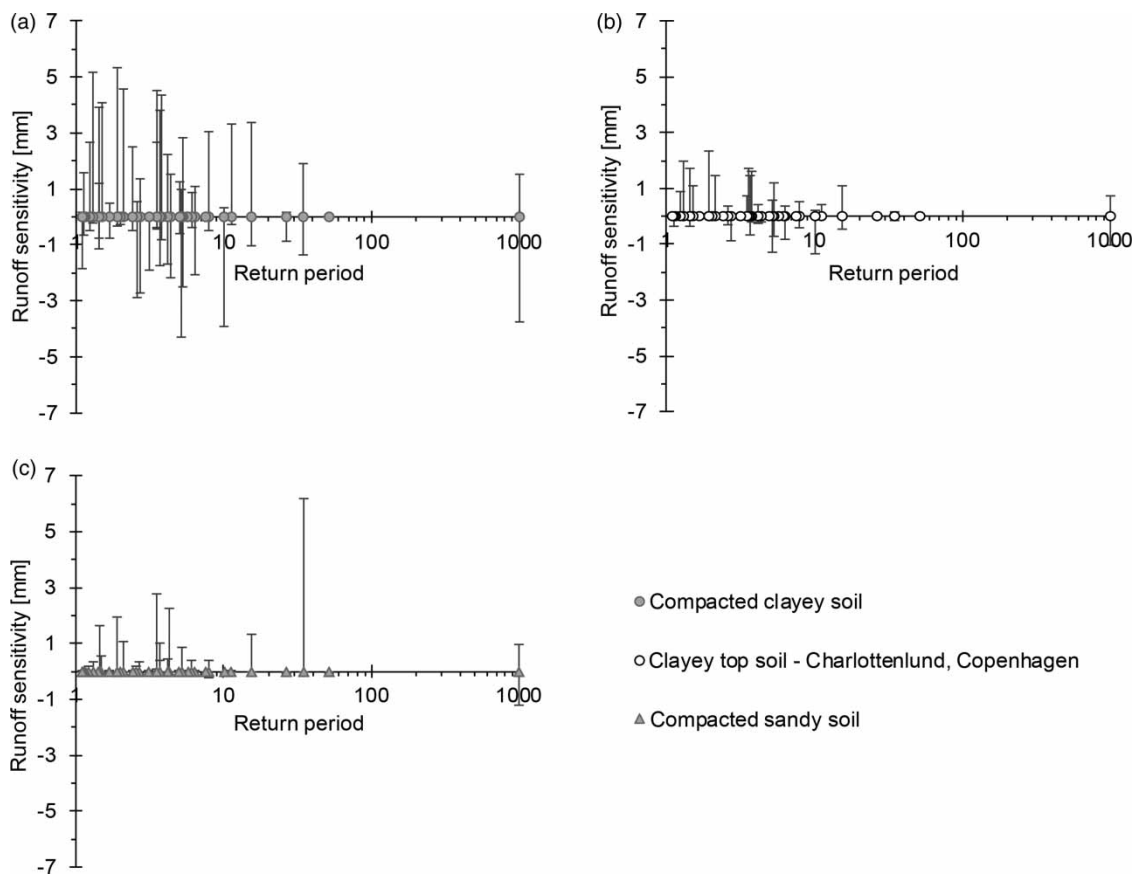


**Figure 4** | Difference between runoff simulated in continuous simulations ( $Q_{tot,acc}$ ) and assuming initial conditions as maximum ( $Q_{tot,min}$ ) or minimum ( $Q_{tot,max}$ ) infiltration capacity for historical rain events. Positive values correspond to  $Q_{tot,max} - Q_{tot,acc}$ , negative values to  $Q_{tot,acc} - Q_{tot,min}$ . Results for (a) compacted clayey soil, (b) clayey top soil and (c) compacted sandy soil.

The employed model gives a somewhat simplistic description of the initial conditions of the runoff and the results in Figure 4 should hence be interpreted with caution. Nevertheless, our results highlight that runoff from green urban areas should not be ignored and that a modelling approach assuming a 'typical' initial condition for a given soil type is a feasible approach to model runoff from high return periods. In addition, we identify a clear need for more measurements of infiltration processes in urban areas.

## CONCLUSIONS

Pervious areas can significantly contribute to the runoff observed during rain events with return periods larger than 5 to 10 years and thus need to be considered in runoff models when designing, for example, climate adaptation measures. The runoff from pervious areas depends on the infiltration conditions in the beginning of an event.

Based on observed precipitation data from Copenhagen, Denmark, an analysis of accumulated rain prior to large rain events shows that the distribution of prior rainfall is independent of the return period and varies only as a function of the considered time span before the event. Considering a period of 7 days prior to a large rain event, it is likely that at least 10 millimetres of rainfall were observed in this period.

Based on continuous simulations of the rainfall-runoff process for a period of 33 years, we demonstrate that initial infiltration capacities of the 40 largest rain events are subject to large variability. The simulations suggest that infiltration capacity in the beginning of an event is significantly reduced for most rain events for both sandy and clayey soils.

The variation in initial infiltration capacity causes changes in the total runoff from clayey soils of up to 6 millimetres at low return periods, though infiltration capacities for these soils are generally small. However, variations in runoff from compacted sand due to different initial

conditions are larger at higher return periods. Maximum runoff rates from both clayey and compacted sandy soils are subject to significant variations, highlighting the importance of making appropriate assumptions for initial infiltration conditions when working with design rainstorms. Both initial conditions and soil types are hence important to assess when designing for return periods higher than 1 year.

## ACKNOWLEDGEMENT

This study, and the work behind it, is completed as a joint project with DTU and LNH Water as part of the WISE project (Water Innovation SmE) funded by the European Regional Development Fund (RFH-15-011) and the Capital Region Denmark (15006962).

## REFERENCES

- Ambjerg-Nielsen, K. & Harremoës, P. 1996 Prediction of hydrological reduction factor and initial loss in urban surface runoff from small ungauged catchments. *Atmospheric Research* **42** (1–4), 137–147. doi: 10.1016/0169-8095(95)00059-3.
- Chahinian, N., Moussa, R., Andrieux, P. & Voltz, M. 2005 Comparison of infiltration models to simulate flood events at the field scale. *Journal of Hydrology* **306**, 191–214. doi:10.1016/j.jhydrol.2004.09.009.
- DHI 2014 *Mouse Runoff Reference Manual. Scientific Documentation*. Danish Hydraulic Institute (DHI), Hørsholm, Denmark.
- Dybkjær, S., Jakobsen, C. C., Petersen, J. A. O. & Rasmussen, R. C. K. 2016 *Infiltration og afstrømning på grønne urbane arealer (Infiltration and Runoff From Urban Green Areas)*. Thesis, Technical University of Denmark, Kongens Lyngby, Denmark.
- Fletcher, T. D., Andrieu, H. & Hamel, P. 2013 Understanding, management and modelling of urban hydrology and its consequences for receiving waters: a state of the art. *Advances in Water Resources* **51**, 261–279. doi:10.1016/j.advwatres.2012.09.001.
- Gregory, J., Dukes, M., Jones, P. & Miller, G. 2006 Effect of urban soil compaction on infiltration rate. *Journal of Soil and Water Conservation* **61**, 117–124.
- Hollander, M. & Wolfe, D. A. 1973 *Nonparametric Statistical Methods*. Wiley, New York.
- Horton, R. E. 1941 An approach toward a physical interpretation of infiltration-capacity. *Soil Science Society of America Journal* **5**, 399. doi:10.2136/sssaj1941.036159950005000C0075x.
- ITWH 2009 *KOSIM 7 Modellbeschreibung (KOSIM 7 Model Description)*. ITWH (Institute for Technical and Scientific Hydrology), Hanover, Germany.
- Leandro, J., Schumann, A. & Pfister, A. 2016 A step towards considering the spatial heterogeneity of urban key features in urban hydrology flood modelling. *Journal of Hydrology* **535**, 356–365. doi:10.1016/j.jhydrol.2016.01.060.
- Madsen, H., Gregersen, I. B., Rosbjerg, D. & Arnbjerg-Nielsen, K. 2017 Regional frequency analysis of short duration rainfall extremes using gridded daily rainfall data as co-variate. *Water Science and Technology* **75** (8), 1971–1981. doi:10.2166/wst.2017.089.
- Ogden, F. L., Raj Pradhan, N., Downer, C. W. & Zahner, J. A. 2011 Relative importance of impervious area, drainage density, width function, and subsurface storm drainage on flood runoff from an urbanized catchment. *Water Resources Research* **47**, 1–12. doi:10.1029/2011WR010550.
- Pitt, R., Lantrip, J., Harrison, R., Henry, C. L., Xue, D. & O'Conner, T. P. 1999 *Infiltration through Disturbed Urban Soils and Compost: Amended Soil Effects on Runoff Quality and Quantity*. US EPA, Cincinnati, OH, USA.
- Pitt, R., Chen, S.-E., Clark, S. E., Swenson, J. & Ong, C. K. 2008 Compaction's impacts on urban storm-water infiltration. *Journal of Irrigation and Drainage Engineering – ASCE* **134**, 652–658. doi:10.1061/(ASCE)0733-9437(2008)134:5(652).
- R Core Team 2015 *R: A Language and Environment for Statistical Computing*. <https://www.r-project.org/>.
- Redfern, T. W., Macdonald, N., Kjeldsen, T. R., Miller, J. D. & Reynard, N. 2016 Current understanding of hydrological processes on common urban surfaces. *Progress in Physical Geography* **40**, 699–713. doi:10.1177/0309133316652819.
- Rossmann, L. A. & Huber, W. C. 2016 *Storm Water Management Model (SWMM) Reference Manual*. US EPA, Cincinnati, OH, USA.
- Verma, S. C. 1982 Modified Horton's infiltration equation. *Journal of Hydrology* **58**, 383–388. doi:10.1016/0022-1694(82)90047-6.

First received 5 October 2017; accepted in revised form 1 November 2017. Available online 16 November 2017